

## 以電腦視覺技術處理平行線資訊做路標定位及其於直昇機自動降落之應用 Using Parallel Line Information for Vision-Based Landmark Location Estimation and an Application to Automatic Helicopter Landing

楊致芳  
Yang Zhi-Fang

交通大學資訊科學系  
Department of Computer and Information Science  
Chiao Tung University, Hsinchu, R.O.C.  
[gis82504@cis.nctu.edu.tw](mailto:gis82504@cis.nctu.edu.tw)

蔡文祥  
Tsai Wen-Hsiang

交通大學資訊科學系  
Department of Computer and Information Science  
Chiao Tung University, Hsinchu, R.O.C.  
[whtsai@cis.nctu.edu.tw](mailto:whtsai@cis.nctu.edu.tw)

### 摘要:

本文提出一種以電腦視覺技術做路標定位的方法，其目的在利用消失點和路標之尺寸以單張影像得知路標相對於車輛之方位。此方法僅需低價之硬體設備及簡易計算。最後我們以直昇機降落區之定位做為一個應用。我們也做了一些模擬及實驗以驗證本方法之可行性。

**關鍵字:** 路標，定位，電腦視覺，平行線，消失點，直昇機降落區。

### Abstract:

An approach to landmark location estimation by computer vision techniques is proposed. Vanishing points and size of the landmark are used to derive the location parameters by a single image. Helicopter landing site location estimation is presented as an application. Simulations and experiments also have been conducted.

**Keywords:** landmark, location estimation, computer vision, parallel lines, vanishing points, helicopter landing site.

### 1. Introduction

Autonomous vehicle navigation is a multi-disciplinary and demanding field. In this field, the location problem [1-8] is most critical. To complete this task, the relative orientation and position between a vehicle and the environment should be obtained. There are two kinds of vision-based approach to solving this problem: the landmark approach [1-4] and the map approach [5-8]. In the second kind of approach, the features extracted from sensor data are matched with the features in a detailed map in the environment to estimate the location parameters.

The estimation of landmark location with respect to a vehicle by computer vision techniques with the aim of low hardware cost and simple computation is the main interest of this study. Emphasis is placed on the study of the automatic detection of the landmark orientation and position. An efficient detection method and a simple computation scheme are proposed.

Related works on landmark detection are surveyed as follows. Sato [1] used an image sequence of the circle of the heliport marking as the visual cue to estimate the position and the altitude of a helicopter with respect to the landing site. It is necessary to know if there is a circle, but the size of the circle need not be known. Chou and Tsai [2] used house corners as the standard mark. Based on the knowledge of the distance from the camera to the ceiling, the relative location between the vehicle and the corner can be uniquely determined. Atiya and Hager [3] used the vertical edges in the environment as the visual landmarks. A stored map was also utilized to compute the robot location by using those correspondences. Gilg and Schmidt [4] developed an approach to landmark-based vehicle guidance in corridors. A symbolic course description is used to specify motion tasks.

In this study, a single image acquired by a camera mounted on the vehicle is used to estimate the landmark position and orientation relative to the vehicle. The vanishing points of the parallel lines extracted from the landmark are detected to derive the landmark orientation. The size of the landmark is used to compute the landmark position. The proposed approach has several advantages. First, the annoying image correspondence problem is not involved. Low hardware cost is required. Finally, the computation is based on the use of analytic formulas and this increases the computation speed and the possibility of hardware implementation.

A case study is presented to estimate landing site location by using the identification marking H defined by the International Civil Aviation Organization (ICAO) [15]. Automatic helicopter landing is highly desired since landing maneuver is one of the most difficult skills demanded of the helicopter pilot. A large

\*This work was supported by National Science Council under Grant NSC-86-2213-E-009-114.

†To whom all correspondences should be addressed.

skills demanded of the helicopter pilot. A large percentage of accidents were attributed to the landing phase of a flight. The proposed approach shows the possibility of automatic detection of the landing site location by computer vision techniques.

In the remainder of this paper, Section 2 includes some definitions used in this study. In Section 3, the derivation of the landmark orientation by the use of the parallel lines extracted from the landmark is described. Section 4 includes the derivation of the landmark position by the use of the size of the landmark. The case study of landing site location estimation by using the proposed approach is described in Section 5. Finally, some conclusions are given in Section 6.

## 2. Problem definition

In this study, it is desired to compute the landmark position and orientation. The landmark position is denoted as  $(x_m, y_m, z_m)^T$ , which is the landmark position with respect to the vehicle. The landmark orientation is denoted as  $\alpha_m$ ,  $\beta_m$ , and  $\gamma_m$ , which represent the angles between the three vehicle body axes and the three main axes of the coordinate system describing the landmark geometry from the viewpoint of the vehicle. In the following, the definitions and notations used in this study are introduced.

Two sets of orthogonal parallel lines are supposed to exist on the landmark. As shown in Fig. 1, they are denoted as line set A and line set B, and each line in line set A is perpendicular to each in B. More specifically, the two sets are  $A = \{A_1, A_2, \dots, A_{p-1}, A_p\}$  and  $B = \{B_1, B_2, \dots, B_{q-1}, B_q\}$ . We use  $p_{ij}$  to indicate that it is the intersection of lines  $A_i$  and  $B_j$ . Also,  $H_i$  is defined to include all the collinear intersections of  $p_{11}, p_{12}, \dots, p_{1(q-1)}$ , and  $p_{1q}$ , and  $V_j$  is all the collinear intersections of  $p_{1j}, p_{2j}, \dots, p_{(p-1)j}$ , and  $p_{pj}$ . For example,  $H_1 = \{p_{11}, p_{12}, \dots, p_{1(q-1)}, p_{1q}\}$  and  $V_2 = \{p_{12}, p_{22}, \dots, p_{(p-1)2}, p_{p2}\}$ . The landmark position is defined as the center point of the square region  $p_{11}p_{1q}p_{pq}p_{p1}$ . This position is chosen to represent the location of the landmark in this study.

Several coordinate systems used in this study are shown in Fig. 2. The camera mounted on the vehicle has a camera coordinate system (CCS), denoted as  $x$ - $y$ - $z$ . The corresponding image plane (ICS) is denoted as  $u$ - $v$ . The three axes of the vehicle body form a vehicle coordinate system (VCS), denoted as  $d_{\text{normal}}$ ,  $d_{\text{lateral}}$ , and  $d_{\text{long}}$ . It is assumed that the line directions of these three body axes in the CCS are pre-known. The global coordinate system (GCS) is also needed, which is denoted as  $x'$ - $y'$ - $z'$ . The  $y'$ -axis and the  $z'$ -axis are set on the ground and parallel to the line sets A and B with the origin located at the center point of the landmark. The landmark position with respect to the vehicle is defined as  $(x_m, y_m, z_m)^T$  which is the center point of the landmark in the VCS. The landmark orientation is defined as  $\alpha_m$ ,  $\beta_m$ , and  $\gamma_m$ , which are the angles between the axes of the

VCS and the GCS with respect to the vehicle, respectively.

The point transformation between the CCS and the VCS is needed to transform the computed landmark position in the CCS into the VCS. This transformation can be found in [17].

## 3. Computing landmark orientation from parallel lines on landmark

As is well known, a 3D line passes through the point  $(p_1, p_2, p_3)^T$  and has the line direction  $(d_1, d_2, d_3)^T$  has a vanishing point  $(u_\infty, v_\infty)^T$  and its line direction can be determined by the vanishing point to be:

$$(d_1, d_2, d_3)^T = \frac{1}{\sqrt{u_\infty^2 + v_\infty^2 + f^2}} (u_\infty, v_\infty, f)^T. \quad (1)$$

where  $f$  is the focal length of the camera and unit length is superimposed on the line direction  $(d_1, d_2, d_3)^T$ . Other findings about vanishing points can be found in [9].

Then, the landmark orientation is computed as follows. At first, the intersections of every two lines in line set A are computed. The coordinates of all intersections are averaged to obtain the vanishing point of line set A. By (1), the line direction of the  $y'$ -axis in the CCS is evaluated and denoted as  $d_y$ . The same process is followed for line set B, and the result is denoted as  $d_z$ . The line direction of the  $x'$ -axis of the GCS in the CCS can be obtained by the cross product of these two line directions,  $d_y \times d_z$ .

Then, the landmark orientation,  $\alpha_m$ ,  $\beta_m$ , and  $\gamma_m$ , can be computed from the inner products of  $d_x$  and  $d_{\text{normal}}$ ,  $d_y$  and  $d_{\text{lateral}}$ , and  $d_z$  and  $d_{\text{long}}$ , respectively, to get the following result:

$$\alpha_m = (d_x \cdot d_{\text{normal}}) / (\|d_x\| \|d_{\text{normal}}\|), \quad (2)$$

$$\beta_m = (d_y \cdot d_{\text{lateral}}) / (\|d_y\| \|d_{\text{lateral}}\|), \quad (3)$$

$$\gamma_m = (d_z \cdot d_{\text{long}}) / (\|d_z\| \|d_{\text{long}}\|). \quad (4)$$

## 4. Computing landmark position from size of landmark

The size of the landmark is used to derive the landmark position in this study. The inter-point distances of all collinear point sets,  $H_i$ 's and  $V_j$ 's, are known in advance. With the inter-point distances, the 3D locations of all collinear points can be computed and used to determine the landmark position.

In the following, we first describe the derivation of 3D point locations of a set of collinear points with known inter-point distances. Next, the derived formulas are used to compute the landmark position.

#### 4.1 Computing 3D locations of collinear points with known inter-point distances

Let the first point of the N collinear points be  $\mathbf{p} = (p_1, p_2, p_3)^T$  and the line direction be  $\mathbf{d} = (d_1, d_2, d_3)^T$ . The N collinear points can be described as:  $\mathbf{p}$ ,  $\mathbf{p} + \delta_1 \mathbf{d}$ ,  $\mathbf{p} + \delta_2 \mathbf{d}$ ,  $\mathbf{p} + \delta_3 \mathbf{d}$ , ..., and  $\mathbf{p} + \delta_{N-1} \mathbf{d}$  where  $\delta_n$  is the distance between the first and the  $(n+1)$ st collinear points. According to the perspective transformation principle, the image point  $(u_n, v_n)^T$  of the  $(n+1)$ st point  $\mathbf{p} + \delta_n \mathbf{d}$  on the image plane can be written as follows :

$$(u_n, v_n)^T = \left( f \frac{p_1 + \delta_n d_1}{p_3 + \delta_n d_3}, f \frac{p_2 + \delta_n d_2}{p_3 + \delta_n d_3} \right)^T, \quad (5)$$

where  $n = 0, 1, \dots, N-1$ . The linear system below is the result of transforming (5) into matrix form for  $n = 0, 1, \dots, N-1$  :

$$\mathbf{A}\mathbf{p} = \mathbf{b}, \quad (6)$$

where

$$\mathbf{A} = \begin{bmatrix} f & \dots & f & 0 & \dots & 0 \\ 0 & \dots & 0 & f & \dots & f \\ -u_0 & \dots & -u_{N-1} & -v_0 & \dots & -v_{N-1} \end{bmatrix}^T,$$

$$\mathbf{p} = (p_1, p_2, p_3)^T,$$

and

$$\mathbf{b} = (\delta_0(u_0 d_1 - f d_1), \dots, \delta_{N-1}(u_{N-1} d_3 - f d_3), \delta_0(u_0 d_3 - f d_2), \dots, \delta_{N-1}(u_{N-1} d_3 - f d_2))^T,$$

where  $\mathbf{p} = (p_1, p_2, p_3)^T$  is the unknowns. In this study, QR-decomposition [11] is used to solve this linear system, which is treated as a least-squares problem. The result is as follows :

if  $q_3 > 0$ , then

$$(p_1, p_2, p_3)^T = \left( \frac{1}{\sqrt{N}f} q_1 + \frac{U}{Nf} q_3, \frac{1}{\sqrt{N}f} q_2 + \frac{V}{Nf} q_3, \frac{1}{q} q_3 \right)^T;$$

otherwise,

$$(p_1, p_2, p_3)^T = -1 \times \left( \frac{1}{\sqrt{N}f} q_1 + \frac{U}{Nf} q_3, \frac{1}{\sqrt{N}f} q_2 + \frac{V}{Nf} q_3, \frac{1}{q} q_3 \right)^T, \quad (7)$$

where

$$(q_1, q_2, q_3) = \left( \frac{1}{N} \sum_{i=0}^{N-1} \delta_i (u_i d_1 - f d_1), \frac{1}{N} \sum_{i=0}^{N-1} \delta_i (v_i d_3 - f d_2), \frac{1}{q} \sum_{i=0}^{N-1} (\delta_i (u_i d_1 - f d_1)(-u_i + \frac{U}{N}) + \delta_i (v_i d_3 - f d_2)(-v_i + \frac{V}{N})) \right)^T$$

$$q = \sqrt{S_U + S_V - \frac{U^2}{N} - \frac{V^2}{N}},$$

$$U = \frac{1}{N} \sum_{i=0}^{N-1} u_i,$$

$$V = \frac{1}{N} \sum_{i=0}^{N-1} v_i,$$

$$S_U = \sum_{i=0}^{N-1} u_i^2,$$

and

$$S_V = \sum_{i=0}^{N-1} v_i^2.$$

#### 4.2 Computing landmark position from sets of collinear points

The point locations of the sets of collinear points,  $H_i$ 's and  $V_j$ 's, are derived as follows. For each collinear point set, suppose that the corresponding line direction in the CCS is  $\mathbf{d} = (d_1, d_2, d_3)^T$ . Assume  $\mathbf{d} = d_1$  for sets  $H_i$ 's and  $\mathbf{d} = d_2$  for sets  $V_j$ 's. Actually, the collinear points can be expressed as  $\mathbf{p}$ ,  $\mathbf{p} + \delta_1 \mathbf{d}$ , ...,  $\mathbf{p} + \delta_{p-2} \mathbf{d}$  and  $\mathbf{p} + \delta_{N-1} \mathbf{d}$ , where  $N = q$  for sets  $H_i$ 's,  $N = p$  for sets  $V_j$ 's, and  $\delta_1, \dots, \delta_{N-1}$  are the inter-point distances for that collinear point set. Now, the location of  $\mathbf{p}$  can be computed directly by (7). Then, the locations of all  $p+q$  collinear point sets can also be computed.

According to our experimental experience, we choose the computed locations of the innermost points of the landmark to evaluate the landmark position. The averaged coordinates of these points are computed to obtain a candidate landmark position. Two candidates positions can be obtained since both sets  $H_i$ 's and  $V_j$ 's are used. The averaged coordinates of them are computed to be the final landmark position in the CCS. Finally, this position is transformed into  $(x_m, y_m, z_m)^T$  in the VCS as the desired landmark position.

#### 5. Case study: landing site location estimation by identification marking for automatic helicopter landing

In this section, a case study of the proposed approach is presented. A single image of the standard identification marking  $\mathbf{H}$  on the helicopter landing site is used to achieve the landing site location estimation. According to the standards adopted by the ICAO [15], an identification marking should be provided on the landing site. As shown in Fig. 3, the identification marking consists mainly of a letter  $\mathbf{H}$ , white in color.  $H_i$  includes all the collinear vertices of  $p_{i1}, p_{i2}, p_{i3}$ , and  $p_{i4}$  on line  $A_i$ , and  $V_j$  includes all the collinear vertices of  $p_{j1}, p_{j2}, p_{j3}$ , and  $p_{j4}$  on line  $B_j$ . The position of the marking is defined as the center point of the cross arm of the  $\mathbf{H}$ . This position is chosen to represent the location of the landing site.

##### 5.1 Landing site location by identification marking

After line set A and line set B are extracted from the acquired image of the identification marking. The process described in Section 3.2 is followed for the estimation of the landing site orientation. At first, intersections of line sets A and B are computed. Next, the corresponding vanishing points and line directions are obtained. After the desired axis directions of the GCS in the CCS,  $d_x$ ,  $d_y$ , and  $d_z$ , are obtained, the landing site orientation,  $\alpha_m$ ,  $\beta_m$ , and  $\gamma_m$  can be computed by Equation (2), (3), and (4).

Eight sets of collinear points,  $H_i$ 's and  $V_j$ 's, can be detected on the identification marking. By (7), the locations of the eight collinear point sets can be computed.

As described in Section 4.2,  $p_{22}$ ,  $p_{23}$ ,  $p_{32}$ , and  $p_{33}$ , are chosen to evaluate the landing site position. The averaged coordinates of two candidates are then computed to be the landing site position in the CCS. Finally, this position is transformed into  $(x_m, y_m, z_m)^T$  in the VCS as the desired landing site position.

## 5.2 Image processing techniques

In this study, sets of parallel lines and sets of collinear points are extracted from the identification marking  $H$  by image processing techniques. The employed methods are described as follows.

For each acquired landing site image, line sets A and B are extracted first by images processing techniques, including thresholding, edge detection, and line detection. Since it is originally a visual aid for the pilot, it is reasonable to pre-select a threshold value to segment the identification marking  $H$  in the image. A computational edge detector [16] yields clean edge points. The Hough transform [10] is applied to the resulting edge points to detect candidate lines. The detected candidate lines are then merged and improved to derive eight lines which can be further divided into two sets of lines. Eight sets of collinear points are then computed. In the following, the identification of line sets A and B from these two sets of lines is described.

The cross ratio [9] is adopted as a feature to recognize line sets A and B from the two detected line sets. By definition, the cross ratio of  $H_i$ 's is 0.082 and the cross ratio of  $V_j$ 's is 0.585. The cross ratio of each line set is calculated and line sets A and B can be recognized by simple comparison of the computed cross ratios and the pre-known cross ratios.

After line sets A and B are found, the detection of the desired elements for the proposed approach is finished.

## 5.3 Experimental results

Simulations have been done to verify the correctness of the formulas derived in this section with noise-free data. The relative errors of the landing site orientation and position are both zero for each test data

set.

Experiments on real images and error analysis have also been conducted. An identification marking satisfying the requirements of the ICAO was made. The proportion of the length is 10:1. Two kinds of measurements are used to compute the error. One is the relative error of the angle between the computed landing site orientations,  $d_y$  and  $d_z$  in the CCS, compared with 90 degrees which is the correct angle. The result is shown in Table 1. The average error is about 3.6 degree. The other is the relative error of the projection of the computed landing site position on the image, the center of the marking, compared with the extracted landing site position in the acquired image. The result is shown in Table 2. The average error is about 1.144 pixel. Both measurements show acceptable results.

## 6. Conclusions

In this study, an approach to estimating the landmark location by computer vision techniques using parallel line information on the landmark is proposed. This approach uses single images to avoid motion analysis which is complicated and time consuming. Only some analytic formulas is needed, which speeds up the estimation process. The vanishing points of the parallel lines of the landmark provide the information for computing landmark orientation. The size of the landmark is used to compute the landmark position. Low hardware cost is also guaranteed since only one camera is required. No equipment on the landmark is needed. No information of the vehicle location or motion is required. In fact, we can compute the vehicle motion by a sequence of landmark location estimation. A case study of the helicopter landing site location for automatic helicopter landing by using the identification marking on the landing site is presented. Acceptable experimental results have been obtained both in simulation and in testing real images.

## References

- [1] M. Sato, "Position and attitude estimation from an image sequence of a circle," *Academic Reports, Faculty of Engineering, Tokyo Institute of Polytechnics*, Vol. 18, Iss. 1, pp. 28-35, 1995.
- [2] H. L. Chou and W. H. Tsai, "A new approach to robot location by house corners," *Pattern Recognition*, Vol. 19, No. 6, pp. 439-451, 1986.
- [3] S. Atiya and G. D. Hager, "Real-time vision-based robot localization," *IEEE Trans. on Robotics and Automation*, Vol. 9, No. 6, pp. 785-800, 1993.
- [4] A. Gilg and G. Schmidt, "Landmark-oriented visual navigation of a mobile robot," *IEEE Trans. on Industrial Electronics*, Vol. 41, No. 4, pp. 392-397, 1994.
- [5] A. D. L. Escalera, L. Moreno, M. A. Salichs, and J. M. Armingol, "Continuous mobile robot

- localization by using structured light and a geometric map," *Int. Journal of System Science*, Vol. 27, No. 8, pp. 771-782, 1996.
- [6] A. Curran and K. J. Kyriakopoulos, "Sensor-based self-localization for wheeled mobile robots," *Journal of Robotic Systems*, Vol. 12, No. 3, pp. 163-176, 1995.
- [7] P. S. Lee, Y. E. Shen, and L. L. Wang, "Model-based location of automated guided vehicles in the navigation sessions by 3D computer vision," *Journal of Robotic Systems*, Vol. 11, No. 3, pp. 181-195, 1994.
- [8] R. Talluri and J. K. Aggarwal, "Mobile robot self-location using model-image feature correspondence," *IEEE Trans. on Robotics and Automation*, Vol. 12, No. 1, pp. 63-77, 1996.
- [9] R. M. Haralick and L. G. Shapiro, *Computer and Robot Vision, Volume II*, Addison-Wesley, New York (1993).
- [10] R. C. Gonzalez and R. E. Woods, *Digital Image Processing*, Addison-Wesley, New York (1992).
- [11] B. Noble and J. W. Daniel, *Applied Linear Algebra*, 3rd Ed., Prentice-Hall, Englewood Cliffs, NJ (1988).
- [12] S. W. Shih, Y. P. Hung, and W. S. Lin, "Accurate linear technique for camera calibration considering lens distortion by solving an eigenvalue problem," *Optical Engineering*, Vol. 32, No. 1, pp. 138-149, Jan. 1993.
- [13] S. Kuo and G. R. Cross, "A string-matching procedure," *Pattern Recognition*, Vol. 24, No. 7, pp. 711-716, 1991.
- [14] M. J. Minneman, "Handwritten character recognition employing topology, cross correlation, and decision theory," *IEEE Trans. Syst. Sci. Cyber.*, Vol. 2, pp. 86-96, Dec. 1966.
- [15] International Civil Aviation Organization, *Aerodromes: ANNEX 14 to the Convention on International Civil Aviation*, Vol. 2: *Heliports*, Montreal, Quebec. International Civil Aviation Organization (1990).
- [16] D. E. Pearson and J. A. Robinson, "Visual communication at very low data rates", *Proceedings of the IEEE*, Vol. 73, No. 4, April 1985.
- [17] L. L. Wang, P. Y. Ku, and W. H. Tsai, "Model-based guidance by the longest common subsequence algorithm for indoor autonomous vehicle navigation using computer vision," *Automation in Construction*, Vol. 2, pp. 123-137, 1993.

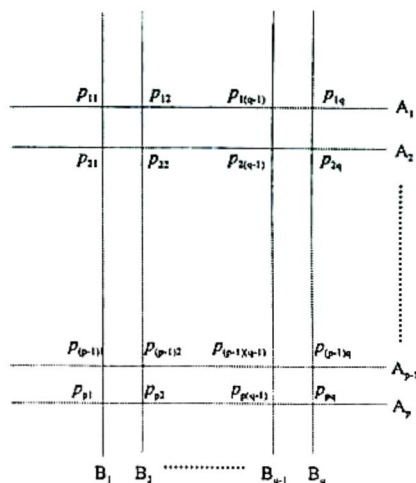


Fig. 1. Illustration of the landmark and the notations used in this study.

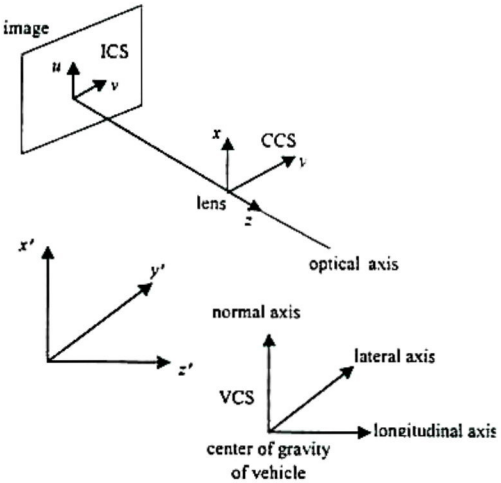


Fig. 2. The camera coordinate system  $x$ - $y$ - $z$ , the image coordinate system  $u$ - $v$ , the global coordinate system  $x'$ - $y'$ - $z'$ , and the vehicle coordinate system.

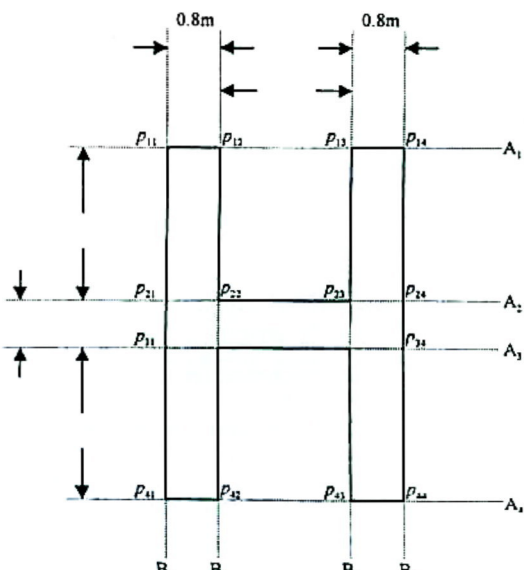


Fig. 3. Illustration of the identification marking  $H$  and the notations used in this study.

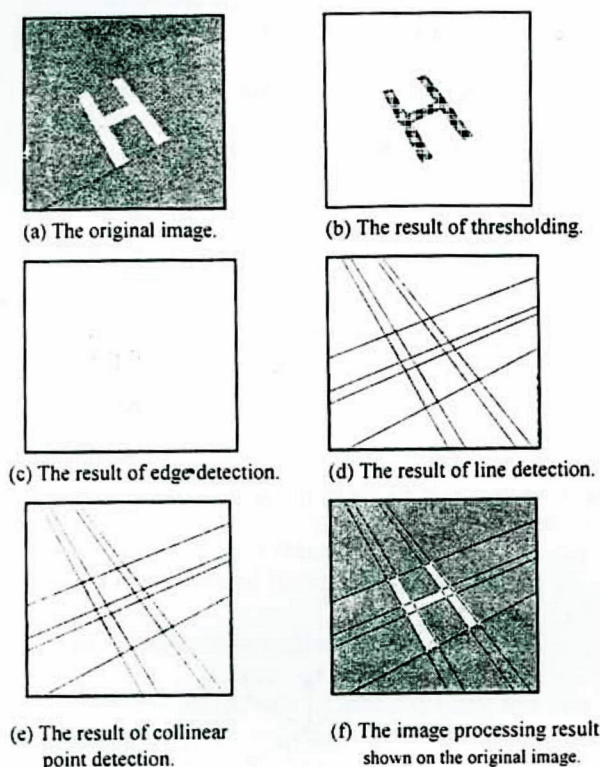


Fig. 4. An image processing result.

Table 1  
Experimental results for landing site orientation.

	computed landing site orientation ( $\alpha_h$ , $\beta_h$ , $\gamma_h$ ) (degree, degree, degree)	Angle between $dy'$ and $dz'$ (degree)	relative error (degree)
1	(44.7933, 152.0871, 50.6771)	88.0102	1.9898
2	(48.8344, 134.9871, 57.6695)	86.6913	3.3087
3	(132.3595, 34.3329, 52.6991)	88.0831	1.9169
4	(127.6449, 54.7279, 57.5232)	84.3886	5.6114
5	(44.9055, 123.8360, 63.2140)	84.7896	5.2104

Table 2  
Experimental results for landing site position.

	computed landing site position ( $x, y, z$ )	projection of computed landing site position ( $u, v$ )	landing site position on acquired image (pixel, pixel) ( $u, v$ )	relative error
1	(44.7933, 152.0871, 50.6771)	(263.59, 248.07) (249.27)	(263.27, 249.27)	(0.32, 1.20)
2	(48.8344, 134.9871, 57.6695)	(240.48, 230.65) (240.94, 231.11)	(240.94, 231.11)	(0.54, 0.46)
3	(132.3595, 34.3329, 52.6991)	(257.86, 220.51) (259.57, 222.93)	(259.57, 222.93)	(2.71, 2.42)
4	(127.6449, 54.7279, 57.5232)	(202.97, 245.76) (203.99, 246.89)	(203.99, 246.89)	(1.02, 1.13)
5	(44.9055, 123.8360, 63.2140)	(294.03, 257.86) (295.18, 257.37)	(295.18, 257.37)	(1.15, 0.49)

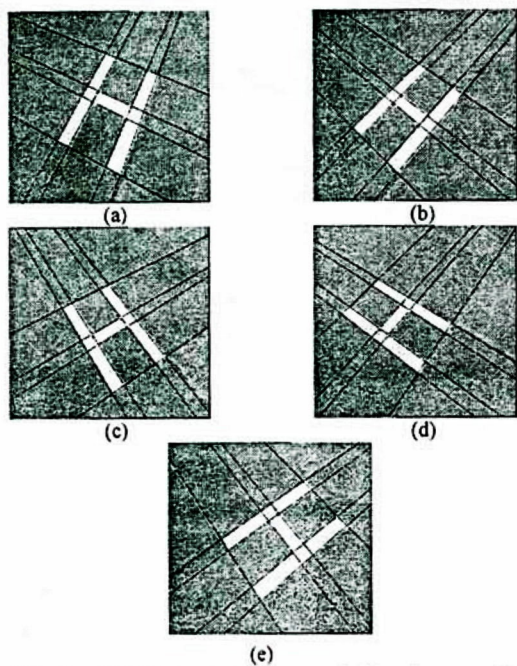


Fig. 5. Projections of the computed four inner vertices of the marking used to evaluate the landing site position on the original images. The white points shows the results computed by the collinear points  $H_i$ 's and  $d_i$ 's, and the black ones by  $V_i$ 's and  $d_i$ 's.